A Passive Ranging Technique for Objects within the Marine Surface Layer

Stephen Doss-Hammel
SSC San Diego

ABSTRACT

Infrared Search and Track (IRST) systems are important to the surface Navy for the detection of low-flying missile threats. Infrared signals propagating within the marine atmospheric surface layer are frequently distorted by strong vertical fluxes. One particular distortion that occurs commonly is the sub-refractive mirage. During sub-refractive mirage conditions, an imaging sensor or camera will record two distinct images of a single point source. A sub-refractive mirage image can be exploited to provide both height and range information. A technique for passive ranging is described, and a case study using field test data is presented as an example of the concept.

INTRODUCTION

Infrared Search and Track (IRST) systems are designed to operate within the marine atmospheric surface layer. This environment can be difficult for radar systems. A reliable passive infrared (IR) system has the potential to provide useful target detection data.

However, the near sea surface environment can also distort images in the infrared. In particular, refraction effects have a strong effect on IR systems, and the occurrence of mirages is not uncommon. This report describes work to exploit one type of mirage, the inferior mirage, to determine range and height of the source creating the mirage image.

REFRACTIVE EFFECTS AND RAY-TRACE TECHNIQUES

The primary computational tool chosen for the analysis of refractive effects was a widget-based simulator called IRWarp that predicts refractive effects [1]. IRWarp uses meteorological conditions as input data for a ray-trace module [2]. The ray-trace data are used to generate detailed information about geometrical transformations induced by the propagation environment.

The ray-tracing method used within IRWarp is from a model by Lehn [3]. The radius of curvature r of a ray is given by:

$$r = \frac{nT^2}{\alpha(\lambda)(T\rho g + p\,dT/dz)} \qquad (1)$$

where T = absolute temperature, ρ = density, p = pressure, g = gravitational acceleration, n = refractive index, and $\alpha(\lambda) = (77.6 + 0.584/\lambda^2)\times 10^{-6}$ for wavelength = λ. It is also assumed that the ray slope does not exceed 10 milliradians.

The formulation in Eq. (1) applies to visible and infrared wavelengths. Pressure A is relatively constant for the measurements made, and the prime determinant of the radius of curvature of near-horizontal rays was the vertical temperature gradient. The ray-trace algorithm first defines the vertical temperature profile as a set of discrete layers, each with a characteristic temperature gradient and refractivity gradient. A characteristic radius of curvature is then assigned to each layer using Eq. (1).

The vertical temperature profile is based upon a surface-layer similarity theory developed by Monin and Obukhov. For the current study, an approach was followed based upon bulk methods for calculating turbulence

parameters described by Davidson et al [4]. Field measurements were taken at the sea surface, and at a reference height, and these values were used to determine the particular values of the scaling parameters. Thus, the sea surface temperature would be T_0 , and the temperature $T(z)$ at a height z above the water surface would be given by

$$T = T_0 + T_*\left[\frac{\ln(z/Z_{0T} - \psi_T(z/L)}{\alpha_T k}\right]$$

where Z_{0T} is the roughness length for the temperature profile, T_* is the potential temperature scaling parameter, and α_T is the ratio of heat transfer to momentum transfer at the surface. L is the Monin–Obukhov length, and $\psi_T(z/L)$ is a stability correction function.

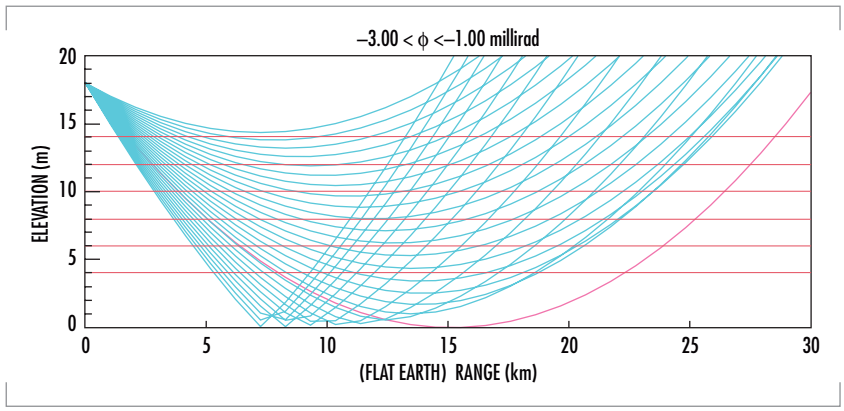

FIGURE 1. The vertical scale is in meters above the surface, while the horizontal scale is in kilometers downrange from the sensor (height = 18 m). The six red horizontal lines indicate level surfaces. The rays that appear to be reflecting from the x-axis are actually refracted.

A ray trace can be generated from the temperature profile by determining a characteristic radius of curvature for each horizontal layer using Eq. (1). Figure 1 displays the traced rays from the ray-trace algorithm for a coordinate system transformed so that the sea surface is the flat x-axis. The figure shows a ray-trace generated from field test temperature profile data. The air–sea temperature difference was ≈–3.5 K. The number of rays has been reduced to make the graphic more legible. The apparent kinks in some of the more sharply bent rays are an artifact; the actual path for the ray is a carefully determined smooth curve, but points on the path are saved only intermittently as needed for the calculation.

An atmospheric surface layer for which the air–sea temperature difference is negative exhibits a crucial feature: the rays form a local coordinate system starting at some point downrange. The logarithmic temperature profile ensures that lower elevation rays are deflected to intersect upper elevation rays. The existence of a locally non-degenerate coordinate system implies that in some region of range-height space there exists a one-to-one correspondence with an upper elevation–lower elevation pair that is unique to that point.

TRANSFORMING IMAGE ELEVATION TO HEIGHT-RANGE DATA

The set of rays tracing the propagation path defines an envelope. The ray envelope has an intersection structure with a set of constant-height surfaces (see Figure 1) at heights of 4, 6, 8, 10, 12, and 14 m. A ray traced from the receiver intersects a given constant-height surface either once, twice, or not at all. The intersection structure of the constant-height surfaces with the ray-trace envelope induces a transformation.

To understand transformation more completely, consider Figure 2. The term "isomet" (isomet surface ≡ surface of constant height) is used to

refer to the contour curves representing the intersection set between a constant-height surface and the ray-trace envelope shown in Figure 2. Each of the isomets in Figure 2 displays a similar form. The vertical axis shows angular displacement from the horizontal tangent plane at the sensor. The horizontal axis shows range.

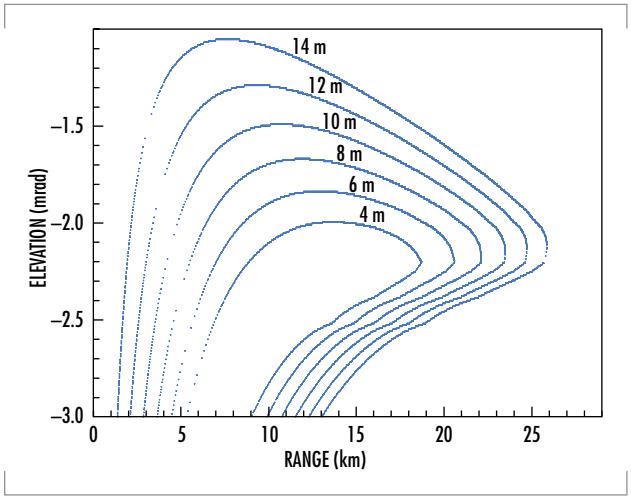

FIGURE 2. A series of isomets at the heights of 4, 6, 8, 10, 12, and 14 m. For a given range value, each isomet defines either 0, 1, or 2 corresponding elevation values.

The graph of a single isomet can be interpreted by imagining a source confined to one of the isomet surfaces (for example, the 14-m isomet) and moving toward the sensor from the 30-km range. At ≈26 km, the source appears over the horizon as a single point that immediately splits into two images. As seen through an imaging sensor, for example, one image decreases in angular elevation, and the upper image increases in angular elevation as the source moves closer in range. At ≈13 km, the lower image descends below –3 milliradians; in terms of the imaginary sensor, it has descended beneath the lowest edge of the sensor focal plane. The (now solitary) upper image continues to rise to the upper edge of the sensor field of view. Within the last 6 km, the source is seen to rapidly move from near the top edge to disappear below the bottom edge.

This form for the 14-m isomet is characteristic of all the isomet contours for surfaces of height less than the sensor height. When the isomet surface height is greater than sensor height, an inbound upper image disappears across the upper boundary, and never re-crosses from top to bottom.

The key to a deduction of height and range from angular elevation information is the utilization of those portions of an isomet for which two values of elevation correspond to a single range value. Thus, for the 14-m isomet, ranges between 13 km and 25 km correspond to two distinct elevation values. This indicates that it is possible to find a one-to-one correspondence between a pair of elevation angles, and a height-range pair.

Thus, the central result in this paper is the transformation shown in Figure 3. When a sensor detects two images, the elevations of the lower and upper images can be plotted as a point in Figure 3, and the height and range of that point can be read from the inner coordinate system. To say it differently, the figure contains the transformation that takes two elevation measurements as input, and generates as output both height and range of the source or target. In terms of coordinate systems, the rectilinear lower elevation vs. upper elevation coordinate system is transformed to the distorted, curvilinear height vs. range coordinate system.

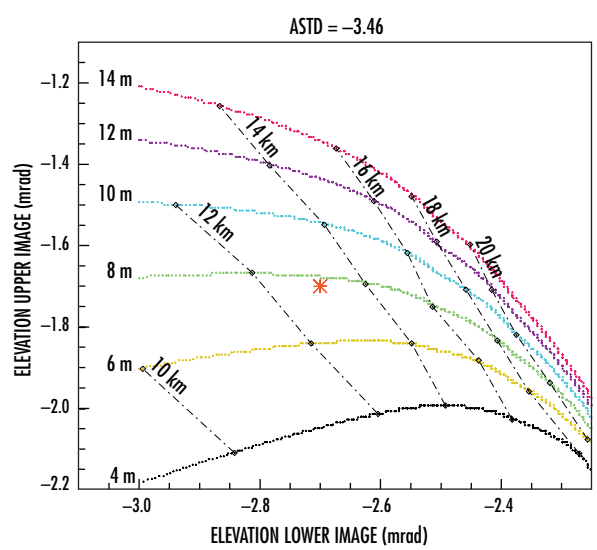

FIGURE 3. The transformation that is implied by the data in Figure 2. The same information is shown here, but restricted to the portions of the isomets that are dual-valued. The point $(\theta_{lower}, \theta_{upper}) = (-2.7, -1.7)$ is plotted as an example, and it transforms to range ≈ 13 km, height ≈ 7.5 m.

Consider as an example an imaging sensor system with a telescope that detects a source in a

sub-refractive mirage regime. The two elevations can be determined from the imaging frame: suppose $(\theta_{lower}, \theta_{upper}) = (-2.7, -1.7)$. This example is plotted in Figure 3. Using the transformation, the actual range and height can be read out from the transformed coordinate system, yielding range ≈13 km and height ≈7.5 m.

SUMMARY

Sub-refractive conditions are quite common for the marine atmospheric surface layer. These conditions cause mirages that appear at two different elevations. These two elevations can be transformed by means of a ray-trace technique to yield height and range information.

The usable range for the particular example presented here is from 10 or 12 km out to ≈20 km. Note that the range limits for effective range-finding are determined by the intensity of the sub-refractive conditions. As air–sea temperature difference $T_{air} - T_{sea}$ becomes more negative, the range domain for which two images occur increases in extent by moving the point of first appearance of two images closer to the sensor. Conversely, as air–sea temperature difference $T_{air} - T_{sea}$ becomes less negative and closer to zero, the range domain for which two images occur decreases in extent; the first appearance of two images occurs at a point farther away from the sensor.

Numerous issues remain to be explored. It is necessary to define the limits of applicability for the method. It is also necessary to establish a mathematical foundation for assumptions made concerning the behavior of surfaces and the intersections between them. Furthermore, the method uses an implicit assumption of homogeneity: the full propagation range is characterized by one vertical profile. This appears to be a reasonable assumption for the sub-refractive case, but this also must be carefully examined. To make practical use of the passive ranging technique, it is important to calculate the limits to the angular elevation resolution.

REFERENCES

1. Hammel, S. and N. Platt. 1995. "Topological Description of Mirage Effects," *Proceedings of the Vision Geometry Conference*, SPIE, vol. 2573, pp. 398–406.
2. Platt, N., S. Hammel, J. Trahan, H. Rivera. 1996. "Mirages in the Marine Boundary Layer—Comparison of Experiment with Model," *Proceedings: IRIS Passive Sensors*, vol. 2, pp. 195–210.
3. Lehn, W. 1985. "A Simple Parabolic Model for the Optics of the Atmospheric Surface Layer," *Applied Math. Model*, vol. 9, p. 447.
4. Davidson, K., G. Schacher, C. Fairall, and A. Goroch. 1981. "Verification of the Bulk Method for Calculating Overwater Optical Turbulence," *Applied Optics*, vol. 20, p. 2919.

❖

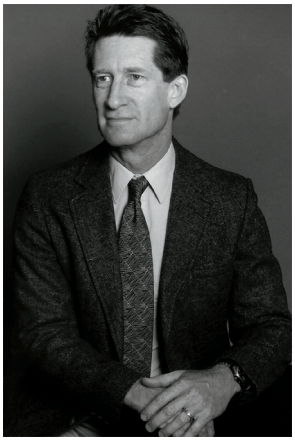

Stephen Doss-Hammel

Ph.D. in Applied Mathematics, University of Arizona, 1986

Current Research: Atmospheric optics and dynamical systems.